Linear pressure waves in bubbly liquids: Comparison between theory and experiments

Kerry W. Commander
Physical Acoustics Branch, Naval Coastal Systems Center, Code 2120, Panama City, Florida 32407

Andrea Prosperetti
Department of Mechanical Engineering, The Johns Hopkins University, Baltimore, Maryland 21218

(Received 1 June 1988; accepted for publication 28 October 1988)

Recent work has rendered possible the formulation of a rigorous model for the propagation of pressure waves in bubbly liquids. The derivation of this model is reviewed heuristically, and the predictions for the small-amplitude case are compared with the data sets of several investigators. The data concern the phase speed, attenuation, and transmission coefficient through a layer of bubbly liquid. It is found that the model works very well up to volume fractions of 1%–2% provided that bubble resonances play a negligible role. Such is the case in a mixture of many bubble sizes or, when only one or a few sizes are present, away from the resonance frequency regions for these sizes. In the presence of resonance effects, the accuracy of the model is severely impaired. Possible reasons for the failure of the model in this case are discussed.

PACS numbers: 43.35.Bf, 43.30.Ft, 43.20.Fn

INTRODUCTION

Although a number of models for the propagation of nonlinear pressure waves in bubbly liquids are available in the literature, it is only recently that a mathematically rigorous derivation of suitable averaged equations has been given by Caflisch *et al.*[1] In their range of applicability, these averaged equations differ only in some quantitatively unimportant terms from those proposed some time ago by van Wijngaarden on the basis of heuristic considerations,[2] and in the linear case they reduce to the pioneering results of Foldy.[3] Another pertinent recent development is a nonlinear formulation suitable for a precise description of the internal dynamics of the bubbles.[4] The combination of these two developments constitutes, therefore, the first rigorously derived mathematical model for the propagation of nonlinear pressure waves in a bubbly liquid.

As a step toward the validation of this model, in the present article we wish to examine in its light the available experimental data on linear pressure wave propagation and attenuation in liquids containing small concentrations of gas bubbles. For the sake of completeness, we also include a brief heuristic, nonrigorous derivation of the theoretical formulation.

The data we consider span a large range of bubble radii, from about 5 μm to 3 mm, and frequencies, from 20 Hz to 10 MHz. The gas volume fractions are, however, all small, from 10^{-5} to 10^{-2}. The picture that emerges from this study is that theory and data agree very well provided that resonance effects are not important, as is the case at all frequencies for bubble size distributions without sharp peaks, or away from the resonance frequency of bubbles in cases in which one or more bubble sizes are predominant. With resonance effects, the agreement between theory and data is less satisfactory even at extremely low gas volume fractions. In the final section, we offer some comments on these results.

I. THE VAN WIJNGAARDEN–PAPANICOLAOU MODEL

We begin with a review of the van Wijngaarden–Papanicolaou model presenting a heuristic, rather than rigorous, derivation for the sake of a greater physical insight.

The continuity equation of the model reads

$$\frac{1}{\rho c^2}\frac{\partial P}{\partial t}+\nabla\cdot\mathbf{u}=\frac{\partial \beta}{\partial t}, \tag{1}$$

where ρ and c are the density and speed of sound of the host liquid, and β is the local fraction of volume occupied by the gas given by

$$\beta=\tfrac{4}{3}\pi R^3 n, \tag{2}$$

where R is the instantaneous radius of the bubbles and n is their number per unit volume. As will be shown presently, n must be kept constant in taking the time derivative indicated in (1). This equation is written for the case in which all the bubbles have the same equilibrium radius. Its extension to different bubble sizes is straightforward and is considered later. The bubbly medium is to be described in an average sense and P and $\mathbf{u}$ indicate the average pressure and velocity. Although ensemble averaging is conceptually the most satisfactory way to define these quantities, volume averaging may be referred to for a simple visualization.

Equation (1) can be justified as follows. Let ρ_m and $\mathbf{u}$ denote the average local mixture density and center-of-mass velocity. Then, we can write an equation for the conservation of total mass of the mixture in the usual form,

$$\frac{\partial \rho_m}{\partial t}+\nabla\cdot(\rho_m\mathbf{u})=0. \tag{3}$$

In terms of the gas volume fraction β, the average density may be written

$$\rho_m=(1-\beta)\rho+\beta\rho_G, \tag{4}$$

where ρ_G is the gas density or, since $\rho_G \ll \rho$,

 0001-4966/89/020732-15$00.80

$$\rho_m \simeq (1-\beta)\rho. \tag{5}$$

Upon substitution into (3) and rearrangement, we have

$$\frac{1}{\rho}\frac{d\rho}{dt} + \nabla\cdot\mathbf{u} = \frac{1}{1-\beta}\frac{d\beta}{dt}, \tag{6}$$

where d/dt denotes the convective derivative. When β is small, the denominator in the right-hand side can be taken as 1 up to order β^2. Furthermore, expanding $d\beta/dt$, we find a term proportional to dR/dt and a term proportional to dn/dt. To estimate this second term, we note that, in the absence of fragmentation or coalescence, the bubble number density must satisfy a conservation equation of the form

$$\frac{dn}{dt} + n\nabla\cdot\mathbf{u}_B = 0,$$

where $\mathbf{u}_B$ is the average velocity of the bubble field. Using this to eliminate dn/dt in (6), we have

$$\frac{1}{\rho}\frac{d\rho}{dt} + \nabla\cdot\mathbf{u} = 4\pi n R^2\frac{dR}{dt} - \beta\nabla\cdot\mathbf{u}_B.$$

Since $\mathbf{u}_B$ must be of the same order as $\mathbf{u}$, the second term in the right-hand side is $O(\beta)$ smaller than the corresponding term in the left-hand side and can be neglected. Furthermore, if ω and λ are a typical frequency and wavelength of the waves, we may write

$$\frac{\partial\beta}{\partial t} \sim \omega\Delta\beta, \quad |\nabla\beta| \sim \frac{\Delta\beta}{\lambda}, \tag{7}$$

where $\Delta\beta$ is the oscillation amplitude of β. With these estimates, we have

$$\frac{|\mathbf{u}_B\cdot\nabla\beta|}{|\partial\beta/\partial t|} \sim \frac{|\mathbf{u}_B|}{\omega\lambda} \sim \frac{|\mathbf{u}|}{c_m}, \tag{8}$$

where c_m is the celerity of pressure waves in the mixture. If, aside from the small effect of liquid compressibility, the motion is solely caused by the volume change of the bubbles and if their number is not too large, $|\mathbf{u}|$ can be expected to be small in comparison with c_m and the spatial part of $d\beta/dt$ can therefore be neglected. A similar argument leads to the approximation $d\rho/dt \simeq \partial\rho/\partial t$ so that, in the end, (6) becomes

$$\frac{1}{\rho}\frac{\partial\rho}{\partial t} + \nabla\cdot\mathbf{u} = \frac{\partial\beta}{\partial t}. \tag{9}$$

By use of the acoustic relation $d\rho = c^{-2}dP$, which holds also for the average values because a linear relation between pressure and density is adequate for ordinary liquids over a very wide range, Eq. (9) is seen to coincide with (1).

Again, in terms of average quantities, the momentum equation may be written

$$\frac{\partial}{\partial t}(\rho_m\mathbf{u}) + \nabla\cdot\mathbf{M} = -\nabla P, \tag{10}$$

where $\mathbf{M}$ is the average mixture momentum flux. Using (3), this may be rewritten as

$$\rho_m\frac{\partial\mathbf{u}}{\partial t} + \nabla\cdot\mathbf{M} - \mathbf{u}\nabla\cdot(\rho_m\mathbf{u}) = -\nabla P. \tag{11}$$

The terms quadratic in $\mathbf{u}$ are small for the conditions previously described, and so is $\beta\mathbf{u}$, so that this relation may be approximated by

$$\rho\frac{\partial\mathbf{u}}{\partial t} + \nabla P = 0, \tag{12}$$

which is the momentum equation of the van Wijngaarden–Papanicolaou model. It is easy to prove from this formulation that the order of magnitude of $\mathbf{u}$ is βc_m. The approximations made are, therefore, equivalent to the neglect of terms of order β^2 with respect to terms of order β.

Caflisch *et al.*[1] rigorously prove that the effects due to the relative motion between bubbles and liquid disappear at the order of the approximations introduced in the model, so that the velocity field $\mathbf{u}_B$ of the bubbles drops out of the formulation. Therefore, at this point, only an equation for R is needed to obtain a closed equation set. This equation will be given in the next section. It may be noted that the radius R must be considered as a field variable $R(\mathbf{x},t)$, where the first argument denotes the position of the bubble.

For a mixture containing bubbles of different sizes, we define

$$d\mathcal{N} = f(a;\mathbf{x})da \tag{13}$$

to be the number of bubbles per unit volume with equilibrium radius between a and $a + da$ located in the neighborhood of the point $\mathbf{x}$. Then, the volume fraction β is given, in place of (2), by

$$\beta(\mathbf{x},t) = \frac{4}{3}\pi\int_0^\infty R^3(a;\mathbf{x},t)f(a;\mathbf{x})da, \tag{14}$$

where $R(a;\mathbf{x},t)$ denotes the radius at time t of a bubble located at position $\mathbf{x}$ and having an equilibrium radius a. It should be noted that no time dependence has been indicated for the distribution function since the same argument given above to neglect dn/dt shows that f can be considered constant during the propagation of the waves. With this expression for β, the continuity equation in the form (1) still holds. The momentum equation (12) is also unchanged but, for every $\mathbf{x}$, a separate radial equation must be written for each a.

II. BUBBLE DYNAMICS

For the case of radial motion of a bubble, an equation accounting approximately for the liquid compressibility was given by Keller[5–7] in the form

$$\left(1-\frac{\dot R}{c}\right)R\ddot R + \frac{3}{2}\left(1-\frac{\dot R}{3c}\right)\dot R^2 = \frac{1}{\rho}\left(1+\frac{\dot R}{c}+\frac{R}{c}\frac{d}{dt}\right)(p_B - P), \tag{15}$$

where p_B is the liquid pressure at the bubble interface related to the internal pressure p by

$$p = p_B + \frac{2\sigma}{R} + 4\mu\frac{\dot R}{R}, \tag{16}$$

and σ and μ denote surface tension and the liquid's viscosity. For an isolated bubble, the term P in (15) is defined as the pressure at the position occupied by the bubble if the bubble were absent. It was first realized by Foldy[3] that, in a dilute mixture, to the lowest order in β this quantity coincides with the average pressure defined in the previous section. In this limit, the bubbles do not interact with each other's field, but with the average field. An intuitive justification can be given

as follows. If the liquid quantities are interpreted in a volume-averaged sense, it may be said that the pressure is, at time t, close to $P(\mathbf{x},t)$ nearly everywhere inside the averaging volume centered at $\mathbf{x}$. Large deviations from this value occur only in the immediate neighborhood of other bubbles. Let us now introduce into the averaging volume the bubble for which (15) was written. Since the volume fraction is small, the probability of it ending up near another bubble is negligible. Furthermore, since an averaging volume must contain many bubbles, the effect on P of the addition of the new bubble can also be neglected.

The dots in Eqs. (15) and (16) denote total time derivatives that, for a bubble in a mixture, must be interpreted as convective derivatives. However, the same argument given earlier justifies their interpretation as partial time derivatives. We shall continue to use the dots for simplicity of notation.

To complete the formulation, an equation for the internal pressure p is needed. Following the procedure of Ref. 4, we start from the enthalpy equation in the gas that, using the equation of state of perfect gases, may be written as

$$\frac{1}{\gamma p}\frac{Dp}{Dt}-\frac{\gamma-1}{\gamma p}\nabla\cdot(K\nabla T)+\nabla\cdot\mathbf{v}=0\,, \tag{17}$$

where γ is the ratio of specific heats, K the thermal conductivity, T the temperature, and $\mathbf{v}$ the velocity. If the bubble boundary moves with a velocity much smaller than the speed of sound in the gas, the pressure can be taken as uniform and the convective derivative with the gas velocity Dp/Dt approximately equated to $\dot{p}$. With these approximations, Eq. (17) can be integrated to find an explicit expression for the radial component of the gas velocity

$$v=\frac{1}{\gamma p}\left((\gamma-1)K\frac{\partial T}{\partial r}-\frac{1}{3}r\dot{p}\right). \tag{18}$$

By imposing the kinematic boundary condition $v=\dot{R}$ at $r=R$, this relation becomes an equation for the pressure

$$\dot{p}=\frac{3}{R}\left((\gamma-1)K\left.\frac{\partial T}{\partial r}\right|_R-\gamma p\dot{R}\right). \tag{19}$$

With these results, the temperature field can be obtained from the standard form of the energy equation

$$\rho C_p\frac{DT}{Dt}-\dot{p}=\nabla\cdot(K\nabla T)\,, \tag{20}$$

in which C_p is the specific heat at constant pressure and $\mathbf{v}$ is given by (18).

It may be noted that the equations for $\mathbf{u}$, P, and β, given in the previous section, together with those for the radial motion just presented, constitute a mathematical model valid also for large-amplitude (or, at any rate, not infinitesimal) pressure waves. The mixture equations appear linearized because, when only a few bubbles are present, even large fluctuations of the bubble volumes can only induce modest average liquid velocities.

III. LINEARIZATION

Upon elimination of $\mathbf{u}$ between (1) and (12), with the usual acoustic approximations (i.e., keeping ρ and c constant), we find

$$\frac{1}{c^2}\frac{\partial^2 P}{\partial t^2}-\nabla^2 P=\rho\frac{\partial^2\beta}{\partial t^2}\,. \tag{21}$$

The time derivative of β, given by (14), is

$$\frac{\partial\beta}{\partial t}=4\pi\int_0^\infty R^2\frac{\partial R}{\partial t}f\,da\,, \tag{22}$$

or, in the linear approximation,

$$\frac{\partial\beta}{\partial t}\simeq 4\pi\int_0^\infty a^2\dot{R}f\,da\,, \tag{23}$$

and, similarly,

$$\frac{\partial^2\beta}{\partial t^2}\simeq 4\pi\int_0^\infty a^2\ddot{R}f\,da\,, \tag{24}$$

so that

$$\frac{1}{c^2}\frac{\partial^2 P}{\partial t^2}-\nabla^2 P=4\pi\rho\int_0^\infty a^2\ddot{R}f\,da\,. \tag{25}$$

It can be shown that, in the linear case, the connection between R and p established by the model of Sec. II is a convolution.[8,9] This reduces to a simple proportionality only in the case of sinusoidal motion, to which we therefore confine the analysis from now on. Upon setting

$$R=a(1+X),\quad p=p_0(1-\Phi X) \tag{26}$$

in the linearized form of Eqs. (19) and (20), and assuming a proportionality to $\exp(i\omega t)$, one readily finds that[4,10]

$$\Phi=\frac{3\gamma}{1-3(\gamma-1)i\chi[(i/\chi)^{1/2}\coth(i/\chi)^{1/2}-1]}\,, \tag{27}$$

where

$$\chi=D/\omega a^2, \tag{28}$$

and D is the gas thermal diffusivity. Note that the function Φ is complex. The quantity p_0 in Eq. (26) is the undisturbed pressure in the bubble given by

$$p_0=p_\infty+2\sigma/a,$$

where p_∞ is the equilibrium pressure in the liquid. With the further definition

$$Q=P-p_\infty\propto\exp(i\omega t), \tag{29}$$

the linearized form of the Keller equation (15) is

$$-\omega^2a^2X=\frac{1}{\rho}\left(1+i\frac{\omega a}{c}\right)\times\left[\left(-p_0\Phi+\frac{2\sigma}{a}-4\mu i\omega\right)X-Q\right]. \tag{30}$$

The derivation of (15) given in Ref. 7 shows that, as an approximation to the equations for a compressible liquid, Eq. (15) has an error of order c^{-2}. On the basis of this remark, it is expedient to multiply (30) by $(1-i\omega a/c)$ and to neglect terms of order c^{-2}. The final result is

$$X=-(\omega_0^2-\omega^2+2ib\omega)^{-1}(Q/\rho a^2), \tag{31}$$

where the definitions

$$\omega_0^2=\frac{p_0}{\rho a^2}\left(\mathrm{Re}\,\Phi-\frac{2\sigma}{ap_0}\right), \tag{32}$$

$$b=\frac{2\mu}{\rho a^2}+\frac{p_0}{2\rho a^2}\,\mathrm{Im}\,\Phi+\frac{\omega^2 a}{2c}, \tag{33}$$

have been introduced to render explicit the similarity of the

bubble response to that of a linear oscillator having a natural frequency ω_0 and a damping constant b. However, the dependence of these quantities on the frequency ω of the pressure wave renders this similarity somewhat superficial. The three terms contributing to the damping constant arise from viscous, thermal, and acoustic effects, respectively. The thermal contribution is normally dominant and it exhibits a strong dependence on ω, particularly near the true resonance frequency.[10,11]

Upon substitution of (31) into the wave equation (25), we obtain

$$\nabla^2 Q + k_m^2 Q = 0, \tag{34}$$

where the wavenumber in the mixture k_m is given by the dispersion relation

$$k_m^2 = \frac{\omega^2}{c^2} + 4\pi\omega^2 \int_0^\infty \frac{af(a)da}{\omega_0^2 - \omega^2 + 2ib\omega}. \tag{35}$$

The complex sound speed in the mixture is given by $c_m = \omega/k_m$ and, therefore,

$$\frac{c^2}{c_m^2} = 1 + 4\pi c^2 \int_0^\infty \frac{af(a)da}{\omega_0^2 - \omega^2 + 2ib\omega}. \tag{36}$$

Setting

$$c/c_m = u - iv, \tag{37}$$

we note that

$$\exp(i\omega t - ik_m x) = \exp\left(-\frac{\omega v}{c}x\right)\exp\left[i\omega\left(t - \frac{u}{c}x\right)\right],$$

which shows the phase velocity V of the sound wave to be given by

$$V = c/u, \tag{38}$$

and the attenuation coefficient A in dB per unit length by

$$A = 20(\log_{10} e)(\omega v/c) \simeq 8.68589(\omega v/c). \tag{39}$$

For a monodisperse bubble population with equal equilibrium radius $\bar{a}$, we have

$$f = n\delta(a - \bar{a}), \tag{40}$$

where n is the bubble number per unit volume, and (36) becomes

$$c^2/c_m^2 = 1 + 4\pi c^2 n\bar{a}/(\omega_0^2 - \omega^2 + 2ib\omega). \tag{41}$$

For a discrete bubble distribution containing radii $\{a_j\}$, $j = 1,2,...,N$, we find (41) with the fraction preceded by a summation over j.

At frequencies well below the natural frequency, (41) reduces to

$$\frac{c^2}{c_m^2} \simeq 1 + 4\pi c^2 \frac{an}{\omega_0^2}\left(1 - \frac{2ib\omega}{\omega_0^2}\right). \tag{42}$$

For $\omega \ll \omega_0$, it may be shown that[10,11]

$$\omega_0^2 \simeq \frac{p_0}{\rho a^2}\left(3 - \frac{2\sigma}{p_0 a}\right), \tag{43}$$

$$b \simeq \frac{\gamma - 1}{10\gamma}\frac{p_0}{\rho D} + \frac{2\mu}{\rho a^2}. \tag{44}$$

With these results, and neglecting for simplicity surface tension effects, we find

$$V^2 = c^2/(1 + \beta\rho c^2/p_\infty), \tag{45}$$

$$A = 8.68589(\beta cb\omega^2 a^2 \rho^2/3p_\infty^2). \tag{46}$$

In particular, for values of β that are not too low, (45) reduces to the well-known result

$$V^2 \simeq p_\infty/\beta\rho. \tag{47}$$

IV. TRANSMISSION AND REFLECTION COEFFICIENTS

We now apply the previous results to the case in which a plane acoustic wave propagating in a pure liquid encounters a uniform bubbly mixture delimited by a plane parallel to that of the incident wave.

The first points to consider are the conditions to be satisfied by the pressure and velocity fields at the clear liquid–bubbly mixture interface. Since the boundary of the bubbly mixture is defined by the presence of bubbles, the velocity of the interface coincides with the velocity $\mathbf{u}_B$ of the bubbles. Conservation of mass across the interface therefore requires that

$$\rho(\mathbf{u}^0 - \mathbf{u}_B)\cdot\mathbf{n} = \rho_m(\mathbf{u} - \mathbf{u}_B)\cdot\mathbf{n}. \tag{48}$$

Here, we have indicated with $\mathbf{u}^0$ the velocity of the pure liquid and with $\mathbf{n}$ the unit vector normal to the interface. As was already done in writing the momentum equation (12), to order β^2, ρ_m can be approximated by ρ when multiplying a velocity. Therefore, (48) gives simply

$$\mathbf{u}^0\cdot\mathbf{n} = \mathbf{u}\cdot\mathbf{n}, \tag{49}$$

irrespective of the motion of the bubbles. The momentum flux tensor in the linear theory is just the pressure times the identity tensor, and continuity of the normal momentum therefore reduces to

$$p^0 = P \tag{50}$$

at the interface, where p^0 is the pressure in the clear liquid.

Consider a one-dimensional situation, and let the bubbly mixture occupy the region $0 \leqslant x \leqslant s$. We imagine the incident sinusoidal wave arriving from $-\infty$. In the region $x < 0$, we then have an incident signal, of unit amplitude, and a reflected wave, of amplitude A_-:

$$p_-^0 - p_\infty = \exp(i\omega t - ikx) + A_- \exp(i\omega t + ikx).$$

At the right of the bubbly mixture, $x \geqslant s$, we have a transmitted wave:

$$p_+^0 - p_\infty = A_+ \exp(i\omega t - ikx).$$

In the bubbly mixture, $0 \leqslant x \leqslant s$, we have both a left- and a right-going wave:

$$P - p_\infty = B_- \exp(i\omega t + ik_m x) + B_+ \exp(i\omega t - ik_m x),$$

where $k_m = \omega/c_m$ is the wavenumber in the mixture. The corresponding forms of the velocity fields are readily obtained from the momentum equations, which, in both media, reduce to

$$u = \frac{1}{i\omega\rho}\frac{\partial P}{\partial x} = \mp\frac{k}{\omega}\frac{P - p_\infty}{\rho},$$

for left- and right-going waves, respectively. Here, ω/k is to be identified with the speed of sound c in the clear liquid and c_m in the mixture.

Imposing the boundary conditions at $x = 0$, we find

$$1 + A_- = B_- + B_+,$$

$$(1 - A_-)/c\rho = (B_+ - B_-)/c_m\rho,$$

while, at $x = s$,

$$B_+E_-^m + B_-E_+^m = A_+E_-,$$

$$(1/\rho c_m)(B_+E_-^m - B_-E_+^m) = (1/\rho c)A_+E_-,$$

where we use the notation $E_\pm = \exp(\pm iks)$, the superscript m indicating that k_m appears rather than k.

The system of equations is readily solved with the result

$$A_+ = \frac{\exp(iks)}{\cos k_m s + i/2(c/c_m + c_m/c)\sin k_m s}, \quad (51)$$

$$A_- = \frac{1}{2}\frac{i(c_m/c - c/c_m)\sin k_m s}{\cos k_m s + i/2(c/c_m + c_m/c)\sin k_m s}, \quad (52)$$

$$B_\pm = \frac{1}{2}\frac{(1 \pm c/c_m)\exp(\pm ik_m s)}{\cos k_m s + i/2(c/c_m + c_m/c)\sin k_m s}. \quad (53)$$

The reflection coefficient of the bubbly layer is defined by

$$R = |A_-|^2, \quad (54)$$

and the transmission coefficient by

$$T = |A_+|^2. \quad (55)$$

Note that, due to the absorption of energy in the bubbly mixture (which translates into a complex value of k_m and c_m), $R + T < 1$ unlike the nonabsorptive case. Equations (51)–(53) were originally derived in Ref. 12. In polar form, we write

$$A_+ = T^{1/2}\exp(i\Psi_+), \quad A_- = R^{1/2}\exp(i\Psi_-), \quad (56)$$

where

$$\Psi_\pm = \tan^{-1}(\mathrm{Im}\,A_\pm)/(\mathrm{Re}\,A_\pm). \quad (57)$$

For a thin layer (i.e., $ks \ll 1$, $k_m s \ll 1$), a Taylor series expansion gives

$$A_- \simeq (is\omega/2c)(1 - c^2/c_m^2),$$

or, using Eq. (36),

$$A_- \simeq 2\pi is\omega c \int_0^\infty \frac{af\,da}{\omega^2 - \omega_0^2 - 2ib\omega} \quad (58)$$

and

$$A_+ \simeq (1 - A_-)^{-1}. \quad (59)$$

We do not make the further approximation $A_+ \simeq 1 + A_-$ because it leads to a substantial loss of accuracy near resonance.

For the case of a thin screen containing bubbles all of the same size with a number density n per unit volume, (58) becomes

$$A_- \simeq [2\pi i\omega ca/(\omega^2 - \omega_0^2 - 2ib\omega)]N_s, \quad (60)$$

where $N_s = sn$ is the number of bubbles per unit area of the screen. The result is independent of the actual screen thickness in this limit. Conversely, for s very large, we find $A_+ = B_- = 0$ and

$$A_- = (c_m - c)/(c_m + c), \quad B_+ = 2c_m/(c_m + c). \quad (61)$$

These two expressions are formally identical to the reflection and transmission coefficients at the interface between two semi-infinite fluids having an equal density but different sound speeds.

V. ANALYSIS OF THE DATA

A number of experimental studies on pressure wave propagation in bubbly liquids can be found in the literature.[12–20] Only some of them contain sufficient detail to render a comparison with the previous theory possible. We shall now consider these, in turn, and, at the end, we shall briefly mention some others.

A. Silberman[13]

The study by Silberman,[13] although published in 1957, still appears to be unsurpassed for the control of bubble size and accuracy of the data. It was conducted by establishing standing waves in 6.35-mm-thick steel pipes filled with the gas–water mixture. Most of the data were taken in a 7.5-cm i.d., 1.80-m-long pipe, but a 5-cm i.d., 240-m-long pipe was also used. For small attenuation, the wave phase speed was deduced from the measurement of the distance between pressure antinodes, and the attenuation coefficient from the ratio of the amplitudes at the antinodes. For attenuations so large that the pressure at two successive antinodes could not be reliably measured, the attenuation coefficient was obtained from

$$\log(P_1/P_2)/(x_2 - x_1), \quad (62)$$

where the positions x_1 and x_2 were close to the sound source. No data for the wave celerity could be taken in these cases. The bubbles were produced from hypodermic needles and other small-diameter tubing, and were therefore relatively large, with radii in the range 1–3 mm and some deviation from sphericity. The size was measured photographically. Control of bubble size required the use of small gas flow rates, and the maximum volume fraction in this study was 1%. Bubble size control at the larger volume fractions studied was not as good as at lower volume fractions, but no quantitative statements on this point can be found in this article. The volume fraction was measured by comparing the hydrostatic head in the columm with that in a column of equal height containing pure water. The variable hydrostatic head in the tubes forced Silberman to apply corrections to this data, never amounting to more than 8%. This was not necessary for the large-attenuation data, since all of these were taken near the sound sources.

We show in Fig. 1 the attenuation coefficient—defined by (39)—for the smallest gas volume concentration studied by Silberman, $\beta = 0.0377\%$. Since data at small void fraction are presumably the easiest ones to obtain in the region of large attenuation, this should be a stringent test of the theory. The data shown are for a ranging between 0.994 and 1.07 mm. The solid line is the theoretical result for $a = 0.994$ mm. The narrow maximum occurs in the immediate vicinity of the resonance frequency of the bubbles that, for the radius quoted, is $\nu_0 = 3.26$ kHz. (Here and in the following the resonance frequencies are stated for an ambient pressure of 1 atm.) The agreement is, in general, good except in the immediate neighborhood of resonance, where the largest attenuation measured by Silberman is less than one-third of the

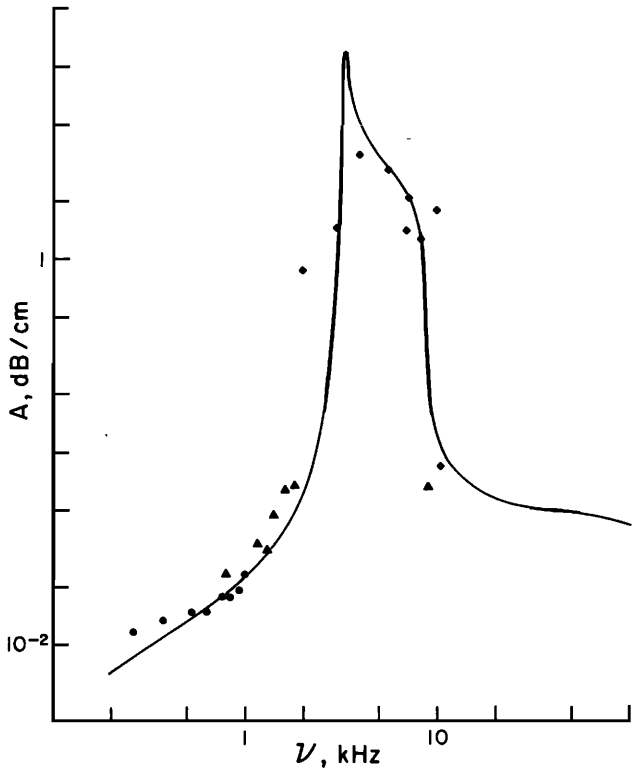

FIG. 1. Comparison between the attenuation coefficient given by Eq. (39) for a bubble radius of 0.994 mm and data from Ref. 13. The volume fraction is 0.0377% and the bubble radii 0.994 mm (diamonds) and 1.07 mm (triangles and circles).

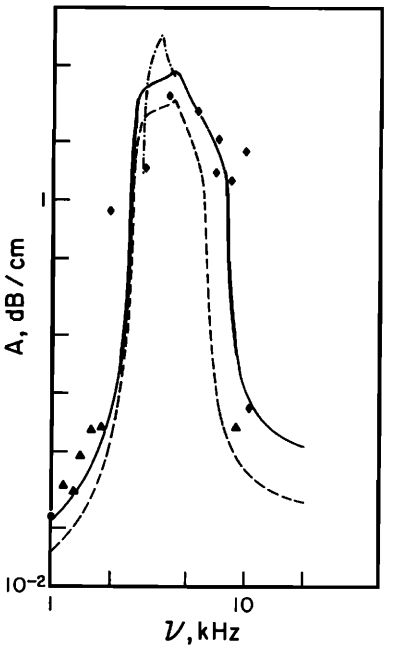

FIG. 2. The same data shown in the previous figure are compared here with the theoretical curves obtained by using the distribution function (63) with $a_0 = 1$ mm, $a_1 = 0.75$ mm, $a_2 = 1.25$ mm, $\sigma_a = 2$ mm, and with $\beta = 0.0377\%$ (solid line) and $\beta = 0.02\%$ (dashed line). The dash-and-dot line corresponds to the same distribution (63) but with a 10% spread in radii and, again, $\sigma_a = 2$ mm, $\beta = 0.0377\%$.

theoretical result. To examine the reasons of this discrepancy and to show the sensitivity of the calculation to the bubble size distribution, we show in Fig. 2 the results obtained by use, instead of a delta distribution, of the truncated Gaussian

$$f(a) = \begin{cases} C \exp[-(a-a_0)^2/\sigma_a^2], & a_1 < a < a_2, \\ 0, & \text{otherwise}, \end{cases} \quad (63)$$

where the constant C is selected to match the prescribed void fraction. The solid line in Fig. 2 shows the results obtained by taking $a_0 = 1$ mm, $a_1 = 0.75$ mm, $a_2 = 1.25$ mm, $\sigma_a = 2$ mm, and $\beta = 0.0377\%$. The dashed line is for the same values of the radius parameters but for $\beta = 0.02\%$. It is clear that, by adjusting these quantities, a significantly better result than that appearing in Fig. 1 can be obtained. However, the amount of adjustment needed is substantial and very likely much greater than the accuracy with which the size distribution and the volume fraction were determined experimentally. This is demonstrated by the dash-and-dot line of Fig. 2, which corresponds to $a_0 = 1$ mm, $a_1 = 0.9$ mm, $a_2 = 1.1$ mm, and $\beta_0 = 0.0377\%$. Evidently a radius spread of 10% is insufficient to lower the maximum attenuation predicted by the theory down to the measured level. We also looked at the possible effect of the hydrostatic head. An increase of the parameter p_∞ by 10% merely displaces the theoretical curves by a very small amount in the direction of increasing frequency, without otherwise affecting their shape.

Figure 3 is for $\beta = 0.22\%$ and the data points have been

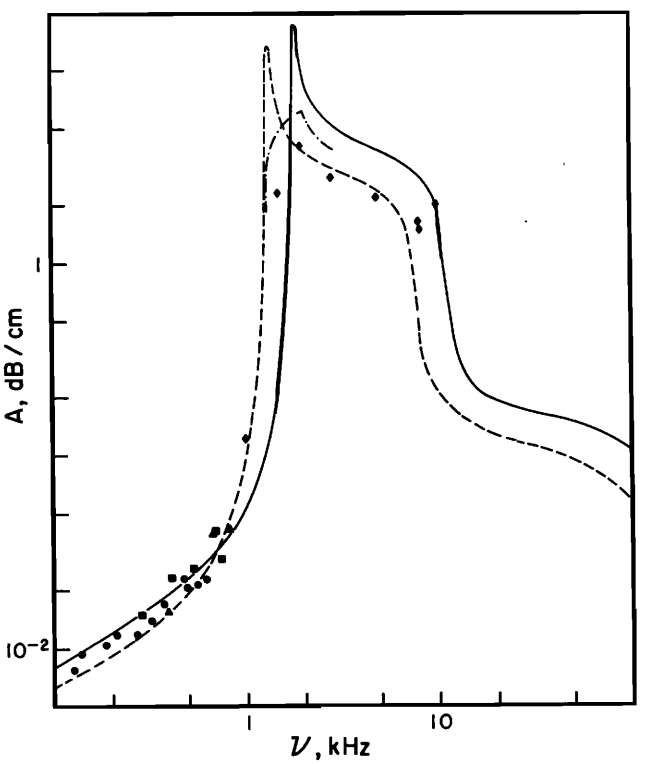

FIG. 3. Comparison between the attenuation coefficient given by Eq. (39) for a bubble radius of 1.77 mm (continuous line) and 2.44 mm (dashed line) and data from Ref. 13. The volume fraction is 0.22% and the bubble radii 1.77 mm (diamonds), 1.83 mm (circles), 2.07 mm (squares), and 2.44 mm (triangles). The dash-and-dot line is obtained with a constant distribution of bubble sizes between 1.77 and 2.44 mm normalized so as to give the correct volume fraction.

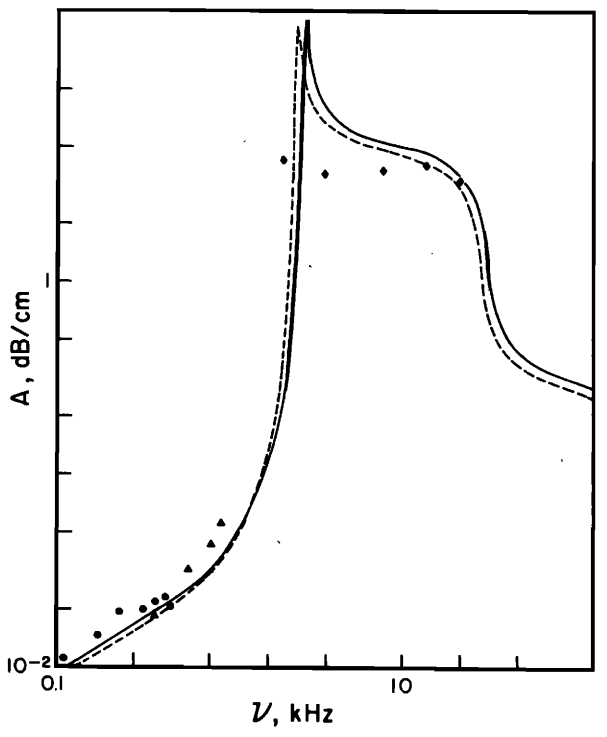

FIG. 4. Comparison between the attenuation coefficient given by Eq. (39) for a bubble radius of 2.07 mm (continuous line) and 2.32 mm (dashed line) and data from Ref. 13. The volume fraction is 0.53% and the bubble radii 2.07 mm (diamonds), 2.13 mm (circles), and 2.32 mm (triangles).

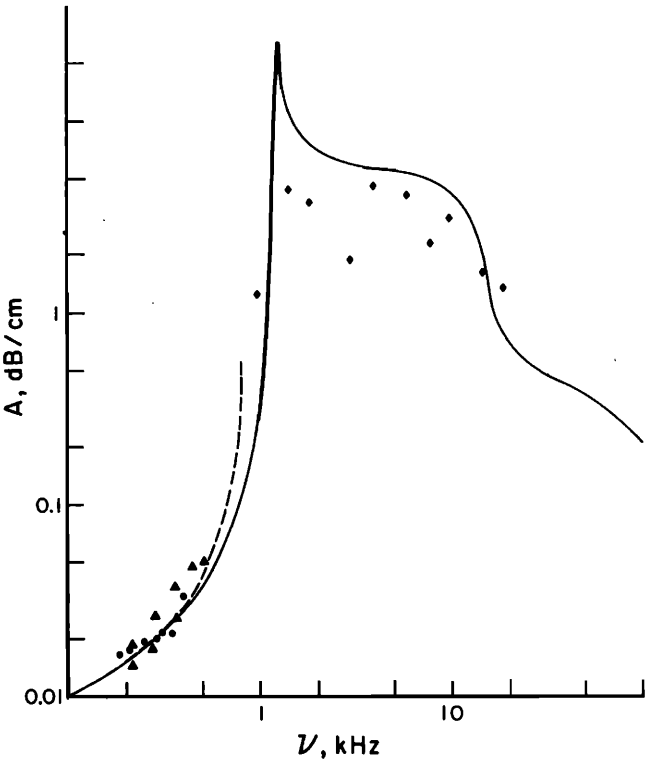

FIG. 5. Comparison between the attenuation coefficient given by Eq. (39) for a bubble radius of 2.68 mm and data from Ref. 13. The volume fraction is 1% and the bubble radii 2.60 mm (diamonds), 2.68 mm (circles), and 3.64 mm (triangles). The dashed line is for a radius of 3.41 mm.

obtained for radii $a = 1.77$, 1.83, 2.07, and 2.44 mm. The continuous theoretical curve has been obtained for $a = 1.77$ mm (resonance frequency $\nu_0 = 1.84$ kHz) while the dashed curve corresponds to $a = 2.44$ mm ($\nu_0 = 1.33$ kHz). The dash-and-dot line has been obtained by use of a constant distribution for 1.77 mm $\leqslant a \leqslant$ 2.44 mm normalized so as to give the correct volume fraction. The data indicated by diamonds should be fitted by the continuous line, but they exhibit the same level of scatter as in the case of the previous figure.

Figure 4 is for $\beta = 0.53\%$ and the data correspond to $a = 2.07$ mm ($\nu_0 = 1.57$ kHz), 2.13 mm ($\nu_0 = 1.53$ kHz), and 2.32 mm ($\nu_0 = 1.40$ kHz). The continuous and dashed theoretical lines are for $a = 2.07$ and $a = 2.32$ mm, respectively. The comparison that emerges from this figure is much like the situation of Figs. 1–3. The agreement is very good in the low-attenuation range but marginal in the resonance region. Very similar conclusions may be drawn from Fig. 5, for which $\beta = 1\%$ and $a = 2.60$, 2.68, and 3.41 mm ($\nu_0 = 1.25$, 1.22, and 0.955 kHz), and from Fig. 6 for the same β but bigger bubbles, $a = 3.42$, 3.45, and 3.54 mm ($\nu_0 = 0.955$, 0.947, and 0.920 kHz). In both these examples, if the very narrow resonance peak is neglected, the discrepancy between theory and the largest measured attenuation is around 30%–50%. The data do, however, exhibit a considerable scatter, particularly in Fig. 5. Finally, Fig. 7 is for a mixture of bubbles with $a = 1.13$ mm ($\nu_0 = 2.87$ kHz) and a β of 0.042% and $a = 2.53$ mm ($\nu_0 = 1.29$ kHz) and a β of 0.0256%. The data are few but the situation similar to that of the preceding examples except for some discrepancy (and

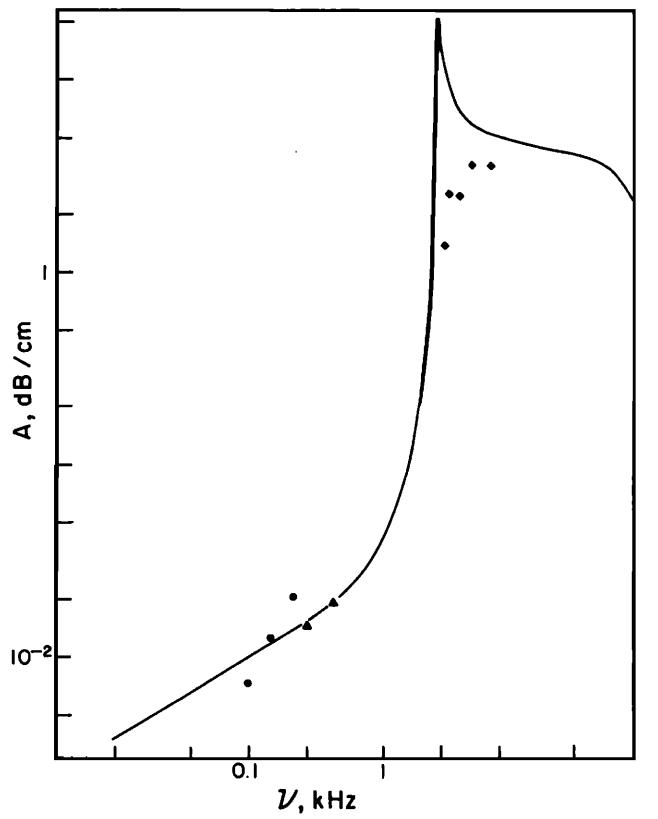

FIG. 6. Comparison between the attenuation coefficient given by Eq. (39) for a bubble radius of 3.416 mm (continuous line) and data from Ref. 13. The volume fraction is 1% and the bubble radii 3.42 mm (triangles), 3.45 mm (diamonds), and 3.54 mm (circles).

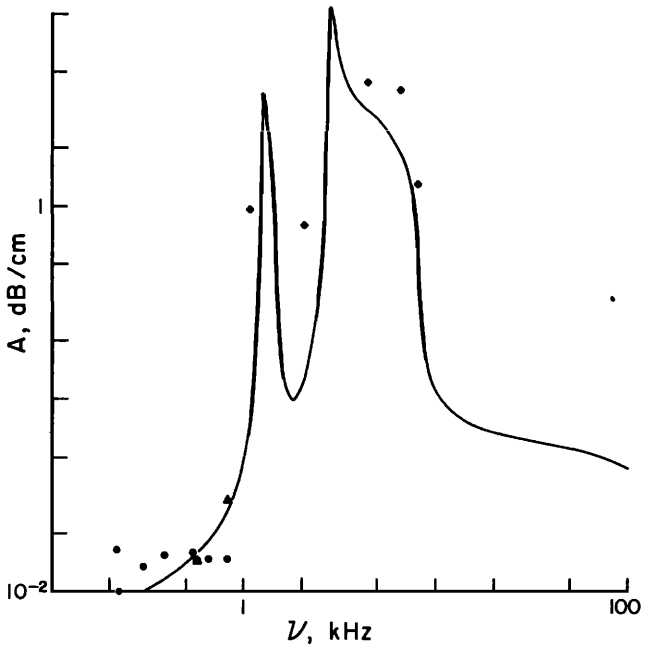

FIG. 7. Comparison between the attenuation coefficient given by Eq. (39) for water containing bubbles with a radius of 1.13 mm, present with a concentration of 0.0421%, and bubbles with a radius 2.53 mm and a concentration of 0.0256%, and data from Ref. 13. The data are for mixtures with radii 1.16 and 2.59 mm (circles and triangles) and 1.13 and 2.53 mm (diamonds).

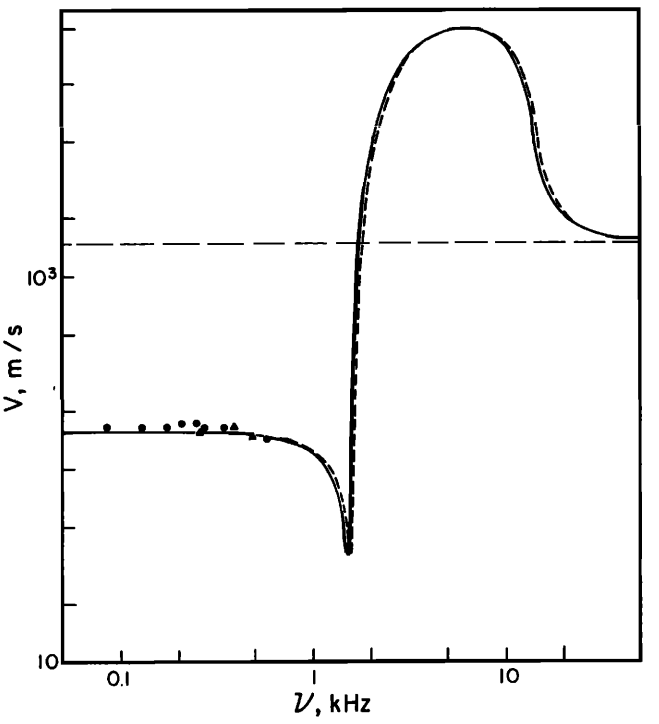

FIG. 9. Comparison between the phase speed of pressure waves given by (38) for a bubble radius of 2.134 mm (continuous) and 2.073 mm (dashed) and data from Ref. 13. The volume fraction is 0.53% and the data are for 2.13 mm (circles) and 2.32 mm (triangles).

experimental scatter) at low frequency.

The next series of figures, from 8–10, shows the phase velocity of the waves. As was already remarked, this could not be measured in the particularly interesting region of high attenuation and, therefore, comparison between theory and experiment, although very good, is not as stringent as might be desired. Only in Fig. 8, for $\beta = 0.0377\%$ and the same conditions as in Figs. 1 and 2, two data points above the region of anomalous dispersion have been obtained, and they agree very well with the theoretical curve.

Silberman compares his data with an approximate theory due to Willis and Spitzer, which gives results very close to

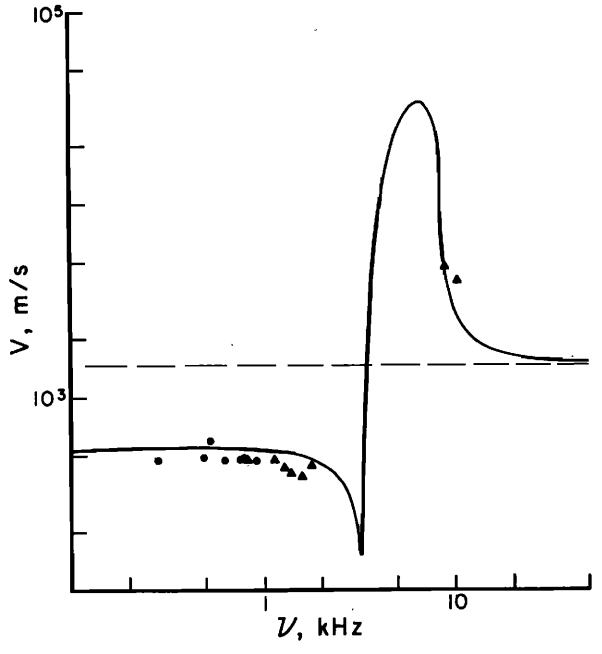

FIG. 8. Comparison between the phase speed of pressure waves given by (38) for a bubble radius of 0.994 mm and data from Ref. 13. The volume fraction is 0.0377% and the data are for 1.07 mm (triangles and circles).

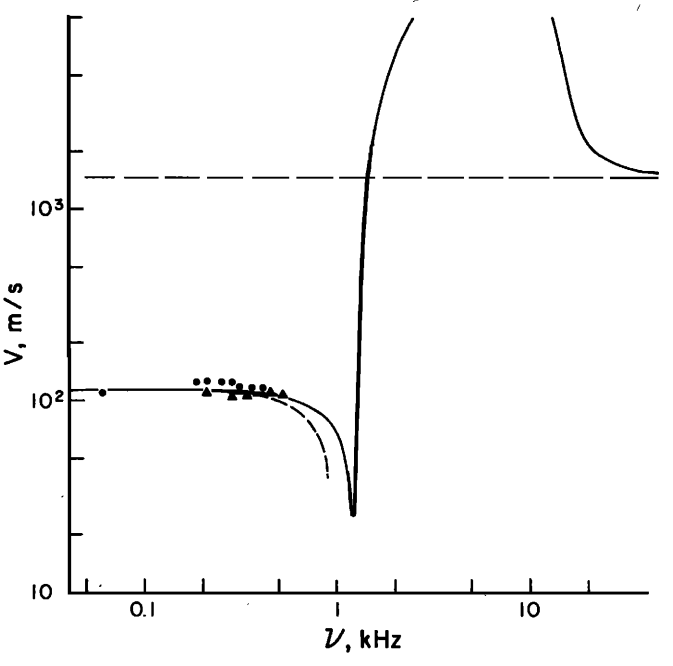

FIG. 10. Comparison between the phase speed of pressure waves given by (38) for a bubble radius of 2.68 mm and data from Ref. 13. The volume fraction is 1% and the data are for 2.68 mm (circles) and 3.64 mm (triangles). The dashed line is for a radius of 3.41 mm.

ours. We have been unable to find the wartime report in which that theory is described. Judging from the formulas quoted by Silberman, this theory assumes the bubbles to behave nearly adiabatically (which is reasonable for the relatively large bubbles of this study) and treats the bubbly mixture in some sort of self-consistent approximation. It, therefore, cannot be expected to be accurate for smaller bubbles, and presumably lacks the solid theoretical foundation of the van Wijngaarden–Papanicolaou model previously described. A close examination of Silberman's results (compare, especially, his Figs. 9 and 4 and our Figs. 1 and 6) shows that the present theory matches the off-resonance data slightly better than his, presumably a consequence of our using a frequency-dependent damping parameter b [see Eqs. (33) and (27)].

B. Fox *et al.*[14]

Another one of the classic studies on pressure waves in bubbly liquids is that of Fox *et al.* published in 1955.[14] In this case, the volume fraction was very small, $\beta = 0.01\%$, but the frequency was higher than in Silberman's work due to the use of smaller bubbles with a radius around 30 μm. These bubbles were produced by blowing air through a 0.6-μm porous porcelain filter. The typical histogram of bubble sizes given in this article is reproduced in Fig. 11. Here, the data have been normalized so that the integral of the distribution gives the reported volume fraction.

In this study, the phase velocity of the waves was measured by comparing the phase of the received signal in a tank containing pure water with that measured in the same tank

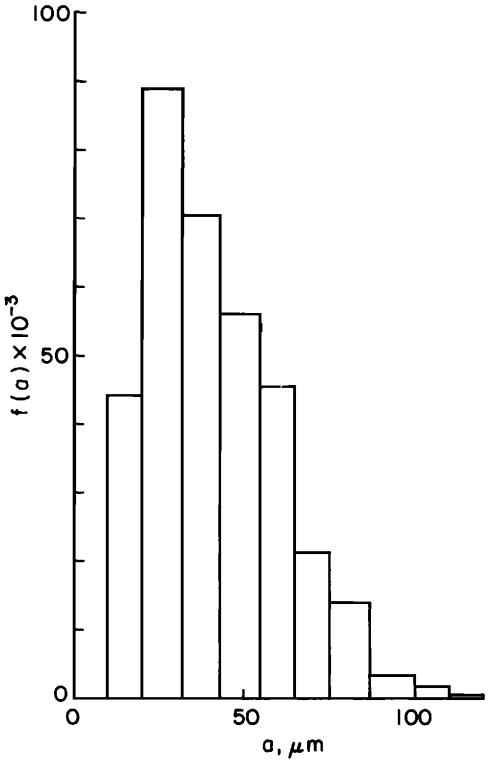

FIG. 11. Histogram of bubble sizes, given as typical in Ref. 14, used in the calculations shown in Figs. 12 and 13.

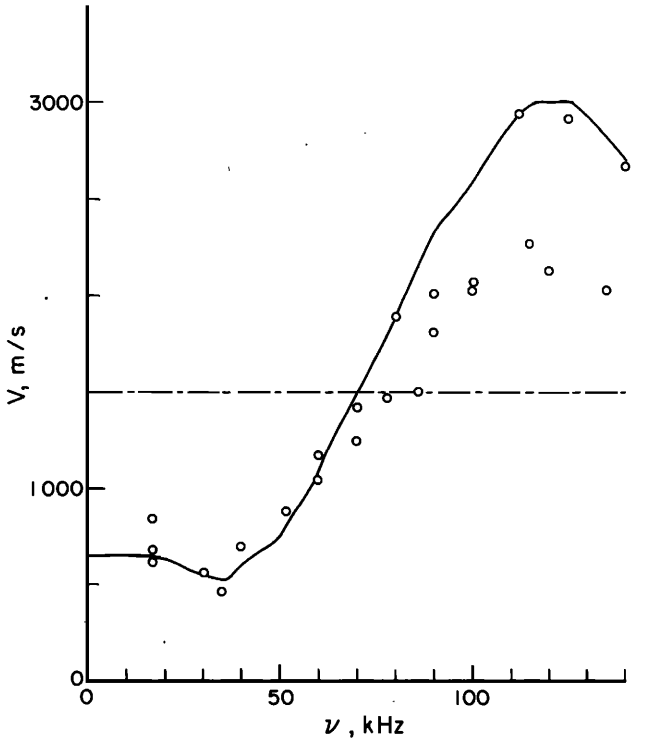

FIG. 12. Comparison between the phase speed given by (38) with the bubble distribution shown in Fig. 11 and the data of Ref. 14. The gas volume fraction is 0.02%. The dashed line is the phase speed in the pure liquid.

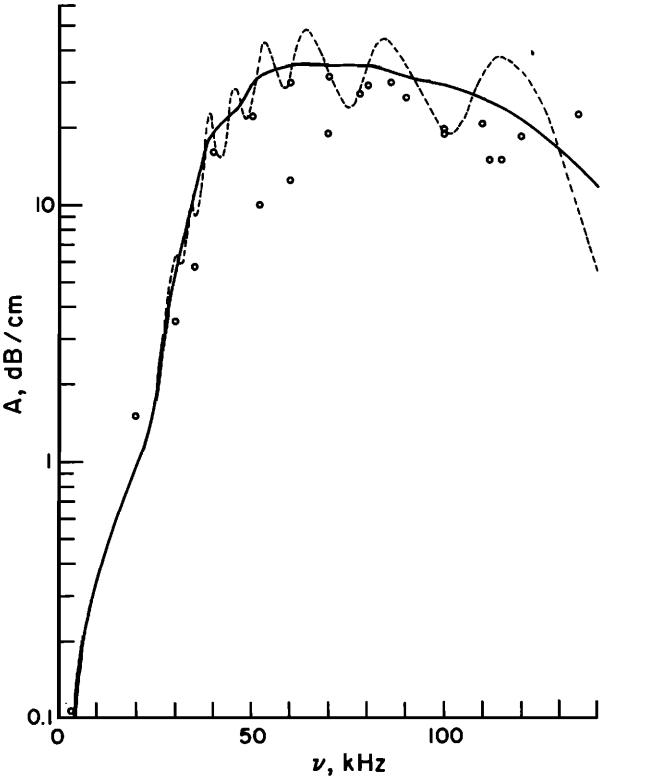

FIG. 13. Comparison between the attenuation coefficient given by (39) with the bubble distribution shown in Fig. 11 and the data of Ref. 14 (continuous line). The gas volume fraction is 0.02%. The dashed line has been obtained by using a bubble distribution consisting of a discrete number of sizes corresponding to the midpoints of the intervals of Fig. 11, rather than the continuous distribution of Fig. 11.

filled with the bubbly mixture. The authors quote an error of 5% for these measurements and an error of 2 dB/cm for the attenuation, which was obtained directly from the amplitude of the measured signal. Fox *et al.* combine, in a single diagram, all their experimental points. The data thus presented exhibit a large scatter, which can be judged from our Figs. 12 and 13. Here, we do not reproduce all the experimental points, but only some chosen so as to bracket the reported data. An example of data obtained in the course of a single experimental run is also given in Ref. 14. Here, the variability is considerably smaller. The authors ascribe these fluctuations to variations in the volume fraction between different runs and to the effect of the standing wave pattern in the tank, which depends on the water level and, therefore, is also subject to change from run to run.

We show in Fig. 12 a comparison between data and theory for the wave speed. The agreement is good below about 70 kHz. In the high-frequency region, although some of the data fall on the theoretical line, the majority of them lie far below. The data on the attenuation coefficient are compared with theory in Fig. 13. Here, the agreement appears to be substantially better, although the data tend to lie slightly below the theoretical line. This result is gratifying since Fox *et al.*, in order to match the data, had to increase substantially the bubble damping calculated on the basis of the limited theory available at the time while no such adjustment has been made on the present theoretical curve.

The data on attenuation are not contaminated by tank resonances, which, therefore, appear to bear the greatest responsibility for the scatter and deviations that affect the phase velocity of Fig. 12. The solid lines shown in the figures have been obtained using the histogram of Fig. 11. The discontinuity of this bubble distribution is reflected in the discontinuity of the slope of these lines. The dashed line in Fig. 13 has been obtained by using a bubble distribution consisting of the superposition of a number of delta functions centered at the midpoints of the histogram. The effect of the continuous distribution in smearing the resonances is evident from the comparison. More interestingly, it is evident that, by introducing the effect of sharp resonances, the theoretical maxima move far above the experimental points much in the same way as was found in the case of Silberman's data. This circumstance seems to imply that the theory is only correct provided resonance effects are not pronounced. We shall return to this point in the final section.

C. Kol'tsova *et al.*[15]

The attenuation data obtained in this article, published in 1979, are unique in the unusually high frequencies that they cover. The use of electrolysis produced very small hydrogen bubbles with a mean size of 15–20 μm. It was found that the bubble spectrum depended somewhat on the liquid temperature and on the gas volume fraction. We reproduce, in Fig. 14, the two histograms given in this article for 15 °C and volume fractions of 0.02% (continuous line) and 0.03% (dashed line), and in Fig. 15 the two histograms for 25 °C and $\beta = 0.005\%$ (continuous line) and 0.025% (dashed line). In the first case, the differences are very minor, while,

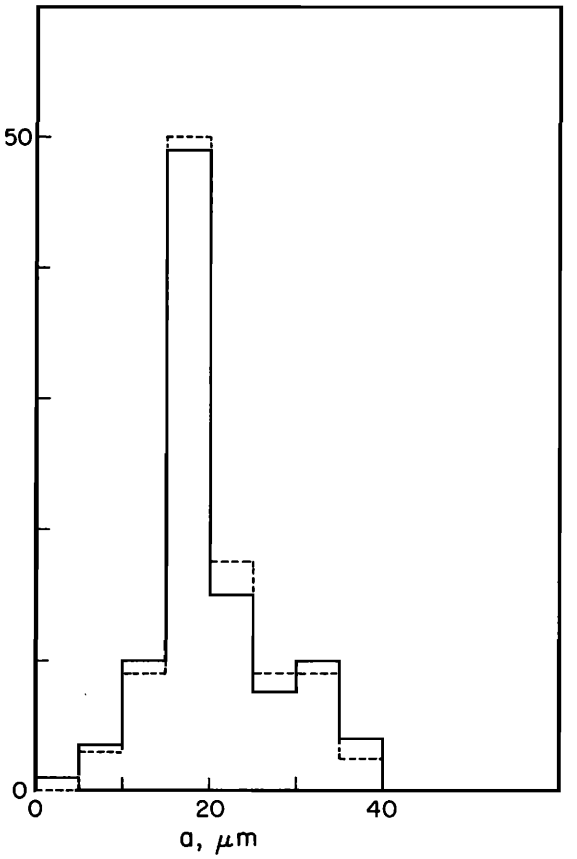

FIG. 14. Histograms of bubble sizes given in Ref. 15 for a liquid temperature of 15 °C and volume fractions of 0.02% (continuous line) and 0.03% (dashed line). The ordinate scale is in arbitrary units (different for the two lines).

in the second case, they are somewhat greater. These bubble distributions were determined photographically or visually with a long-focus microscope. The volume fraction in this study ranged between 0.002% and 0.04%. Only volume fractions greater than 0.02% could be measured directly, the other ones being inferred by extrapolation on the basis of the current in the electrolyzer. No comments are given on the accuracy of this procedure.

The attenuation coefficient was obtained by the use of Eq. (62), plotting the amplitude of pulses at five to ten different separations $x_2 - x_1$. A significant variability (up to 30%) in the attenuation coefficient was observed due to nonuniform spatial distribution of bubbles and fluctuations in the acoustic signal. The data reported are, therefore, averages of an unspecified number of observations. In the frequency range explored, the liquid (a 3% solution of sodium chloride in water) causes some (unspecified, but presumably small) attenuation and the data express the excess attenuation due to the bubbles. The authors give their data in terms of inverse e-folding length, rather than dB per unit length, and this is the quantity that we compare in the figures that follow. The difference between the two is the numerical factor $20 \log_{10} e \simeq 8.68589$ in Eq. (39).

We show in Fig. 16 a comparison between some of the data presented by Kol'tsova *et al.* for a temperature of 15 °C and the present theory. We have selected the data corresponding to $\beta = 0.004\%$ (circles) and $\beta = 0.037\%$ (trian-

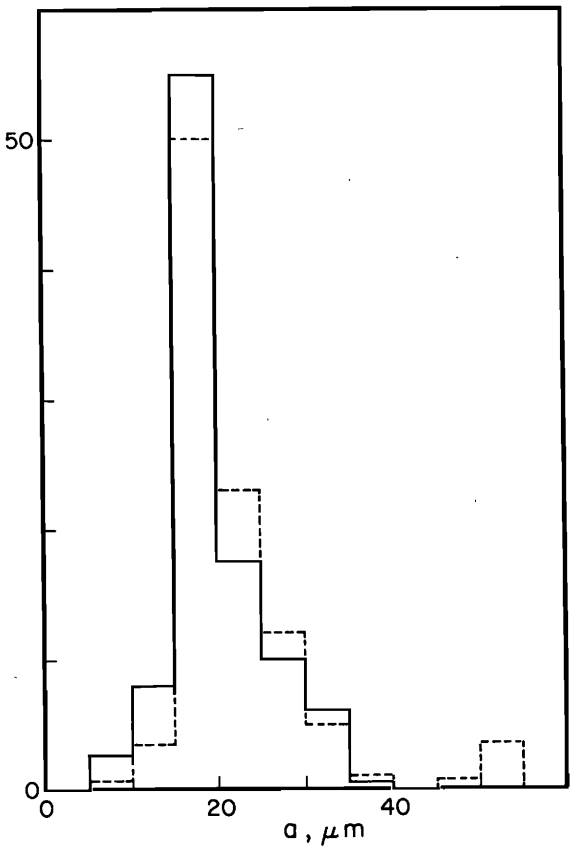

FIG. 15. Histograms of bubble sizes given in Ref. 15 for a liquid temperature of 25 °C and volume fractions of 0.005% (continuous line) and 0.025% (dashed line). The ordinate scale is in arbitrary units (different for the two lines).

gles). The first set corresponds to the largest volume fraction for which a complete set of data also covering the resonance region is given, while the second set corresponds to the largest volume fraction investigated experimentally. In the calculations we have used for both cases, the bubble distribution of Fig. 14 corresponding to $\beta = 0.03\%$ suitably normalized. In the first case, we see a pattern emerging very much like the one previously observed, namely, a general agreement between theory and experiment except in the resonance region, where the data are consistently substantially below the theory. In the second case, the data only cover the high-frequency region, and the discrepancy with the theory increases with increasing frequency. In this high-frequency region, the smaller bubbles in the distribution, which are very difficult to measure, play a dominant role, and it is possible that this is the origin of the disagreement. We have tried to reconcile data and theory by modifying the bubble distribution, but we found that very substantial alterations would have been needed, and we have desisted in view of the arbitrariness involved in this effort.

Figure 17 is for a temperature of 25 °C and $\beta = 0.004\%$ and 0.04%. The criteria with which we selected these data are the same as for the previous figure. For the lower volume fraction case, we have used the distribution function of Fig. 15 corresponding to $\beta = 0.005\%$. Here, the comparison is very similar to that found for Silberman's data in Figs. 1–6 with an overprediction of the data in the resonance region and a reasonable agreement elsewhere. For the higher volume fraction, we have used the bubble distribution of Fig. 15 corresponding to $\beta = 0.025\%$. As in the case of the previous figure, the theoretical curve falls below the data at high frequency, which is again possibly the result of the imprecise measurement of small bubbles. The secondary narrow peak in the theoretical curve is caused by the small number of bubbles with radius between 45 and 55 μm of the distribution used for this case.

Finally, we show in Fig. 18 data and theory for $\beta = 0.002\%$ obtained with the same distribution function of Fig. 15 for $\beta = 0.005\%$ suitably scaled. Here, the discrepancies are very large. Certainly, the data exhibit a large scatter, but this does not seem sufficient to account for the order-of-magnitude differences. At such a low volume fraction, however, the authors were unable to measure directly the bubble distribution and the void fraction, as was mentioned above, and these uncertainties can possibly explain the large differ-

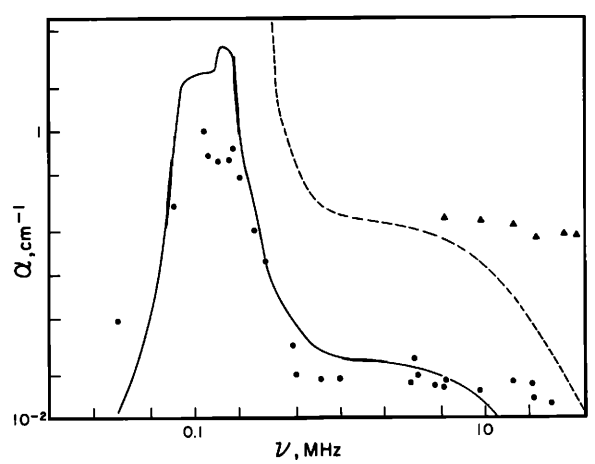

FIG. 16. Comparison between the attenuation length [given by Eq. (39) without the numerical factor 8.68589] for volume fractions of 0.004% (continuous line and circles) and 0.037% (dashed line and triangles) and data from Ref. 15. The theoretical curves have been obtained using the histogram given by the dashed line of Fig. 14.

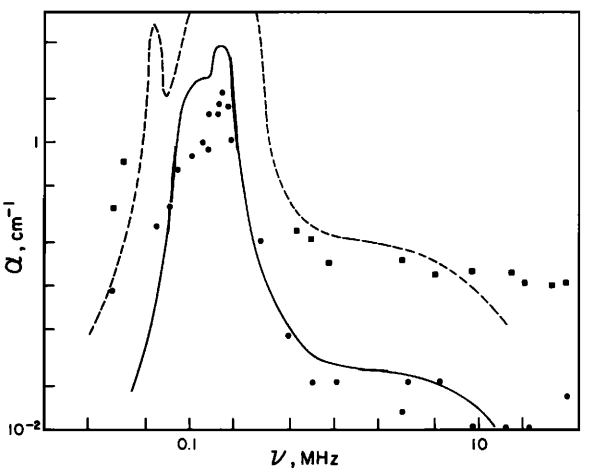

FIG. 17. Comparison between the attenuation length [given by Eq. (39) without the numerical factor 8.68589] for volume fractions of 0.004% (continuous line and circles) and 0.04% (dashed line and triangles) and data from Ref. 15. The continuous and dashed theoretical curves have been obtained using the continuous and dashed histograms Fig. 15, respectively.

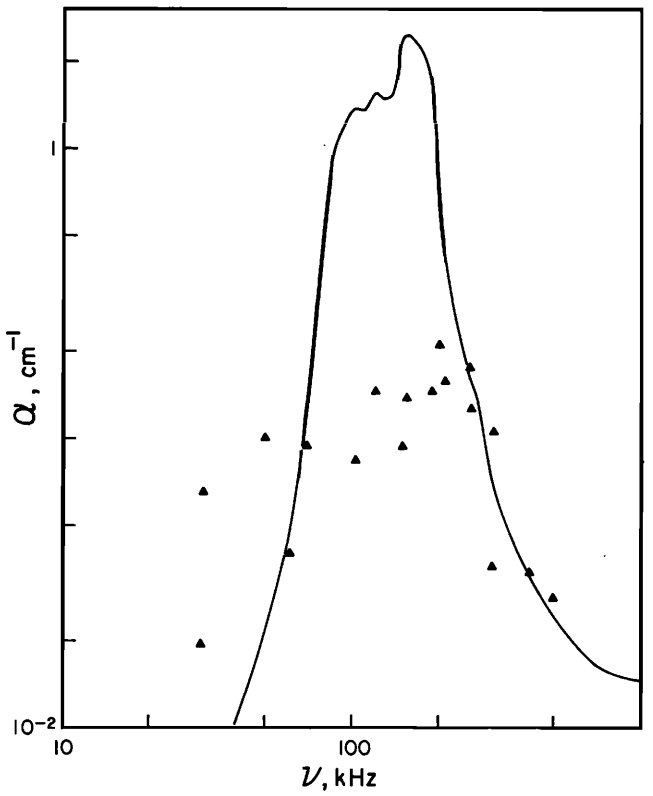

FIG. 18. Comparison between the attenuation length [given by Eq. (39) without the numerical factor 8.68589] for volume fractions of 0.002% and data from Ref. 15. The theoretical curve has been obtained using the histogram given by the continuous line of Fig. 15.

ences observed. It may be recalled from Sec. III that, for small β, the attenuation coefficient is linear in β. It appears, therefore, that, if a reconciliation of theory and experiment is attempted by modifying this quantity, a very large adjustment would be required.

D. Macpherson[16]

These data, published in 1957, are the only ones we consider that are concerned with the attenuation produced by a bubble screen. In this case, oxygen bubbles were produced electrolytically by a row of equal electrodes. By pulsing the current at a certain rate, a two-dimensional lattice of slowly rising bubbles was obtained. The bubble size was determined in a number of ways, including the measurement of their ascending speed, and was found to be nearly uniform with a 7% standard deviation. While the ascending speed is useful to determine relative radii, it is less accurate for an absolute measurement due to the uncertainty with which it can be predicted in the case of bubbles having a size of a fraction of a millimeter. Macpherson states that "the direct photographic method and the measurement of the rate of rise were both found to be less accurate for determining the absolute bubble size than the acoustic method." Here, we have adjusted the bubble size so as to fit the data, and include results for two slightly different sizes to show the sensitivity to this variable.

We reproduce in Fig. 19 Macpherson's data and the theoretical curve for the transmission coefficient through the screen versus frequency. [The quantity plotted is

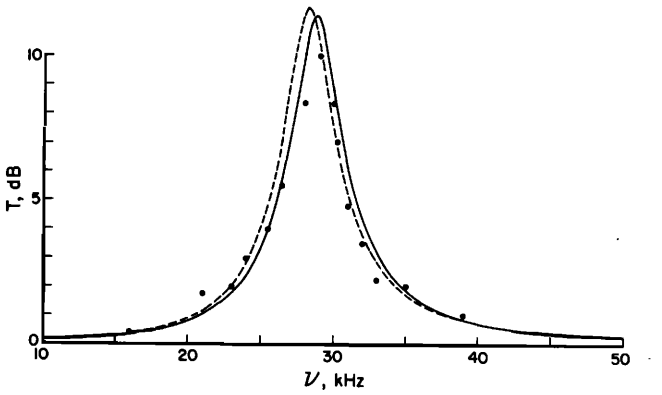

FIG. 19. Comparison between the transmission coefficient given by (55), in decibels, for bubbles with a radius of 0.110 mm (continuous line) and 0.112 mm (dashed line) and data from Ref. 16.

$-10\log_{10} T$, with T defined in Eq. (55).] In Fig. 20, we show data and theory for the phase shift of the transmitted wave defined in Eq. (57). In both figures, the solid lines are for $a = 0.110$ mm ($\nu_0 = 28.7$ kHz) and the dashed lines for $a = 0.112$ mm ($\nu_0 = 28.2$ kHz). This difference is well within the experimental error but it noticeably affects the results. It is interesting to note that the phase data appear to match the theory better than the amplitude data.

E. Ruggles *et al.*[17]

Very recently, Ruggles *et al.*[17] repeated essentially the same experiment conducted by Silberman with similar (if updated) procedures. They investigated gas volume fractions between 0.5% and 18%, bubble radii of the order of 1–2 mm, and frequencies up to about 200 Hz, which is far below resonance for the bubble sizes they used. Their data offer the possibility to investigate the progressive deterioration of the accuracy of the model considered here as the volume fraction increases. An attempt to reproduce their data on attenuation for $\beta = 0.5\%$, which is well within the region explored by Silberman, gives rather poor results. The authors themselves were unable to fit these data with their theory, while they got much better comparisons at higher volume fractions. This circumstance seems to imply that the

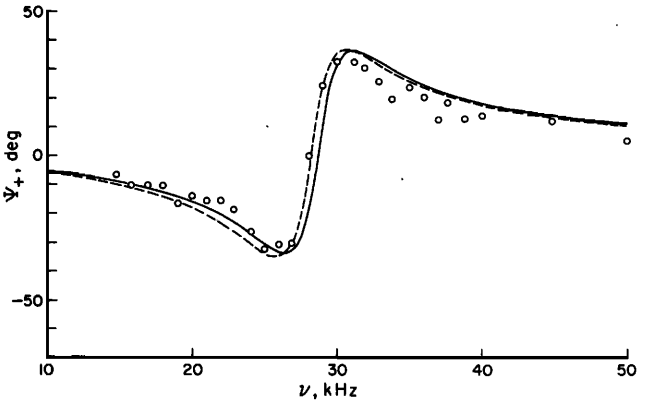

FIG. 20. Comparison between the phase of the transmitted amplitude given by (57) for bubbles with a radius of 0.110 mm (continuous line) and 0.112 mm (dashed line) and data from Ref. 16.

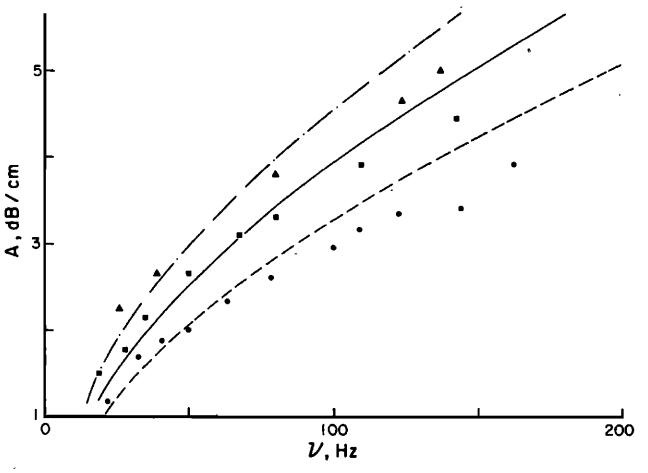

FIG. 21. Comparison between the attenuation coefficient given by (39) and data from Ref. 17. The dashed line and the circles are for a volume fraction of 2.89% and bubble radius of 1.5 mm. The continuous line and the squares are for a volume fraction of 5% and bubble radius of 1.7 mm. The dash-and-dot line and the triangles are for a volume fraction of 10% and bubble radius of 2.2 mm.

low volume fraction data are faulty. A comparison between the present theory and the measured attenuation coefficient for $\beta = 2.89\%$ (average radius 1.5 mm), $\beta = 5\%$ (average radius 1.7 mm), and $\beta = 10\%$ (average radius 2.2 mm) is shown in Fig. 21. Interestingly enough, the numbers predicted are generally within 10% of the measurements, which is a very good and perhaps unexpected finding at these much larger volume fractions.

F. Other data sets

A few other experiments on small-amplitude wave propagation in bubbly liquids exist in the literature. Carstensen and Foldy[12] reported in 1947 the results of tests on bubble screens conducted in a lake. The control of bubble sizes and spatial distribution in these early experiments was rather poor and we felt that it would be next to impossible to compare these data with theory in a meaningful way.

Gibson[18] reports some wave celerity data obtained in a horizontal pipe in the presence of flow. Air was introduced in the water by means of a pipe with no control on bubble size distribution, which is not even mentioned in the article. There was no control on the sound frequency either, and what was measured was essentially the low-frequency speed given by (47) in a range of volume fraction between 0% and 0.8%. We feel that the low-frequency data of Silberman allow a much more stringent and meaningful comparison between theory and experiment.

Medwin[19] reports some data on the attenuation caused by a stream of electrolytically generated bubbles with a radius of 52 μm. It is not clear how to describe this situation in such a way that the present theoretical formulation is applicable, and we have not attempted to do so.

Finally, Card *et al.*[20] report measurements of wave celerity at large volume fractions, up to 40%, and far above resonance (500 kHz with bubbles of a few mm radius). For volume fractions up to 1%–2%, they find a speed essentially equal to that in the pure liquid, which agrees with the predictions of the present model far above resonance (see, e.g., Figs. 8–10). However, their data indicate a decreasing wave celerity at higher volume fractions, which, not surprisingly, cannot be explained by our model. This article also contains a number of references to other measurements contained in unpublished reports and therefore, unfortunately, inaccessible.

VI. CONCLUSIONS

We have analyzed in detail five different sets of data for the propagation of linear pressure waves in a bubbly liquid in the light of a model that, though simple, has a rigorous mathematical basis. For the data sets of Silberman and Kol'tsova *et al.*, who used fairly monodisperse mixtures, we consistently found that the agreement between theory and experiment deteriorates significantly in the neighborhood of the resonance of the bubbles, even at volume fractions as low as a few hundredths of 1%. A corresponding deterioration was not apparent in the comparison with the data obtained by Fox *et al.*, who used bubbles of a relatively wide size distribution, nor with the data of Macpherson, who used two-dimensional bubble screens.

In considering these results, the very dramatic increase of the scattering cross section of bubbles in the neighborhood of resonance comes immediately to mind. The scattering cross section σ_s is defined by[21]

$$\sigma_s = 4\pi a^2 \omega^4 / [(\omega_0^2 - \omega^2)^2 + 4b^2\omega^2]. \tag{64}$$

For example, the ratio of σ_s to the geometric cross section πa^2 for an air bubble in water at 1 atm increases from approximately 752 for $a = 0.1$ mm to 5644 for $a = 1$ mm at $\omega = \omega_0$. On purely intuitive grounds, one may expect that such enormous increases would make the volume fraction "look bigger" than its actual value. This remark can be put on more quantitative grounds in several ways. For example, it is evident that, if the average pressure field exciting a bubble is smaller than, or comparable with, the pressure wave scattered by a neighboring bubble, the model will fail. It is easy to prove that this criterion imposes a limitation of the form

$$(a/d)\omega/|\omega_0^2 - \omega^2 + 2ib\omega| \ll 1, \tag{65}$$

where d is the distance between the two bubbles. If this distance is taken to be the average interbubble distance $n^{-1/3}$, the preceding relation takes the form $n^{2/3}\sigma_s \ll 1$, which can become particularly stringent near resonance.

Other upper limits can be found in the multiple scattering literature. These are pertinent here because it can be shown that the present model, in the linearized approximation, gives results equivalent to those of multiple scattering such as pioneered by Foldy[3] and improved by others since (see, e.g., Refs. 22–27). For example, from the condition that the multiple scattering field caused by the insertion of a bubble be much smaller than the field exciting that bubble, Waterman and Truell[23] derive the condition $n\sigma_s/k \ll 1$ that, in terms of the volume fraction, implies

$$C = a[(\omega_0^2 - \omega^2)^2 + 4b\omega^2]/3c\omega^3 \gg \beta. \tag{66}$$

In Fig. 22, we show the left-hand side of this equation as a function of ω/ω_0 for bubble radii of 1 mm (continuous line),

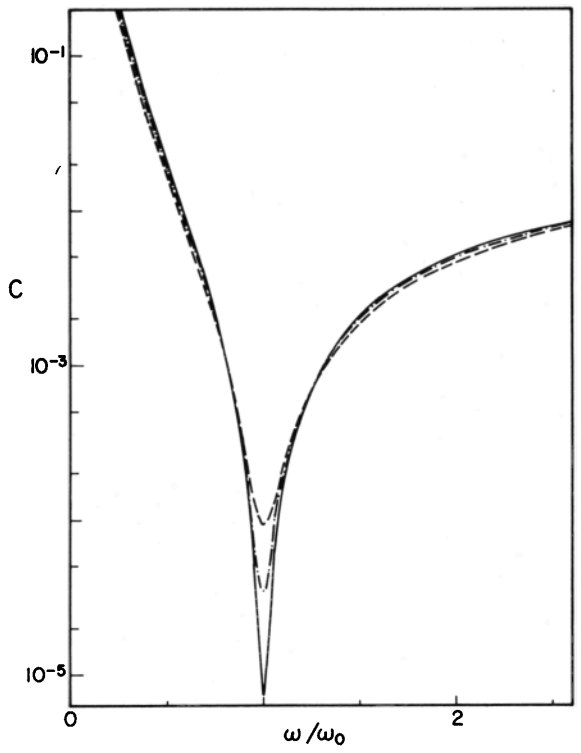

FIG. 22. Graph of the quantity defined in Eq. (66) as a function of the ratio of the driving frequency to the resonance frequency for bubbles with radii of 1 mm (continuous line), 0.1 mm (dash-and-dot line), and 0.01 mm (dashed line). These curves can be interpreted as an upper limit to the volume fraction for the validity of the present theory.

0.1 (dash-and-dot line), and 0.01 mm (dashed line). The extremely severe limitation imposed by this inequality near resonance is particularly striking, and can account for the disagreement between theory and experiment that we have found. Further criteria can be obtained from other multiple scattering studies, such as those of Keller[24] and Twerski.[25–27] Their result can be put in the form

$$na\sigma_s^{1/2} \ll 1 \tag{67}$$

and arises from the condition of negligibility of two-particle correlation effects.

All of these forms point very clearly to the determinant effect of the scattering cross section at resonance. The much better agreement found in the case of the data by Fox *et al.* and Macpherson can perhaps be explained in the light of these considerations by noting that, in the first case, the number of resonant bubbles at any frequency is so small that these stringent limits are met. In the second case, due to the two-dimensional bubble screens used, one deals with a very small volume fraction and, in addition, a peculiar geometry that tends to reduce bubble–bubble interactions.

For the small-amplitude regime to which we have restricted our considerations, more sophisticated treatments than that afforded by the linearization of the model presented in Secs. I and II are available in the literature,[27] and it is conceivable that a better agreement with the data can be obtained by use of some of those results. We have not pursued this matter because the primary motivation of this study was the desire to validate the nonlinear model by a consideration of its restrictions in the linear case. Our conclusion is, therefore, that, since it fails in this case when resonance effects are important, most likely the same will happen for large-amplitude waves. Away from resonance, our results imply that the model performs well up to volume fractions of about 1%–2%. Although this does not, of course, guarantee an equally adequate performance in the nonlinear case, it certainly is an encouraging result.

A number of nonlinear models for pressure waves in bubbly liquids have been proposed that are purported to include many more effects than those contained in the present one such as relative motion of the phases, Reynolds stresses, and others.[8,28–30] All these models, however, have been derived by more or less *ad hoc* procedures. The model we have considered is the only one, to our knowledge, to have a sound mathematical basis and this has been the origin of our interest in it.

ACKNOWLEDGMENTS

The authors are grateful to D. H. Kim and V. Kamath for their help with the data. This study has been supported by the Office of Naval Technology under subproject RJ14M17.

[1] R. E. Caflisch, M. J. Miksis, G. C. Papanicolaou, and L. Ting, "Effective equations for wave propagation in bubbly liquids," J. Fluid Mech. **153**, 259–273 (1985).
[2] L. van Wijngaarden, " On equations of motion for mixtures of liquid and gas bubbles," J. Fluid Mech. **33**, 465–474 (1968).
[3] L. L. Foldy, "The multiple scattering of waves," Phys. Rev. **67**, 107–119 (1945).
[4] A. Prosperetti, L. A. Crum, and K. W. Commander, "Nonlinear bubble dynamics," J. Acoust. Soc. Am. **83**, 502–513 (1988).
[5] J. B. Keller and I. I. Kolodner, "Damping of underwater explosion bubble oscillations," J. Appl. Phys. **27**, 1152–1161 (1956).
[6] J. B. Keller and M. J. Miksis, "Bubble oscillations of large amplitude," J. Acoust. Soc. Am. **68**, 628–633 (1980).
[7] A. Prosperetti and A. Lezzi, "Bubble dynamics in a compressible liquid. Part 1. First-order theory," J. Fluid Mech. **168**, 457–478 (1986).
[8] A. Prosperetti, "A model of bubbly liquids," J. Wave-Mater. Int. **1**, 413–432 (1986).
[9] A. Prosperetti, "Thermal behavior of oscillating gas bubbles," to be submitted to J. Fluid Mech.
[10] A. Prosperetti, "Bubble phenomena in sound fields: part one," Ultrasonics **22**, 69–77 (1984).
[11] A. Prosperetti, "Thermal effects and damping mechanisms in the forced radial oscillations of gas bubbles in liquids," J. Acoust. Soc. Am. **61**, 17–27 (1977).
[12] E. L. Carstensen and L. L. Foldy, "Propagation of sound through a liquid containing bubbles," J. Acoust. Soc. Am. **19**, 481–501 (1947).
[13] E. Silberman, "Sound velocity and attenuation in bubbly mixtures measured in standing wave tubes," J. Acoust. Soc. Am. **29**, 925–933 (1957).
[14] F. E. Fox, S. R. Curley, and G. S. Larson, "Phase velocity and absorption measurements in water containing air bubbles," J. Acoust. Soc. Am. **27**, 534–546 (1955).
[15] I. S. Kol'tsova, L. O. Krynskii, I. G. Mikhalov, and I. E. Pokrovskaya, "Attenuation of ultrasonic waves in low-viscosity liquids containing gas bubbles," Akust. Zh. **25**, 725–731 (1979) [English translation: Sov. Phys. Acoust. **25**, 409–413 (1979)].
[16] J. D. Macpherson, "The effect of gas bubbles on sound propagation in water," Proc. Phys. Soc. London Sec. B **70**, 85–92 (1957).
[17] A. E. Ruggles, H. A. Scarton, and R. T. Lahey, "An investigation of the propagation of pressure perturbations in bubbly air/water flows," in *First International Multiphase Fluid Transients Symposium*, edited by H. H. Safwat, J. Braun, and U. S. Rohatgi (American Society of Mechanical Engineers, New York, 1986), pp. 1–9.
[18] F. W. Gibson, "Measurement of the effect of air bubbles on the speed of

sound in water," J. Acoust. Soc. Am. **48**, 1195–1197 (1970).
[19]H. Medwin, "*In situ* acoustic measurements of bubble populations in coastal ocean waters," J. Geophys. Res. **75**, 599–611 (1970).
[20]D. C. Card, G. E. Sims, and R. E. Chant, "Ultrasonic velocity of sound and void fraction in a bubbly mixture," J. Basic Eng. **93**, 619–623 (1971).
[21]C. S. Clay and H. Medwin, *Acoustical Oceanography* (Wiley, New York, 1977), p. 465.
[22]M. Lax, "Multiple scattering of waves," Revs. Mod. Phys. **23**, 287–310 (1951).
[23]P. C. Waterman and R. Truell, "Multiple scattering of waves," J. Math. Phys. **2**, 512–537 (1961).
[24]J. B. Keller, "Stochastic equations and wave propagation in random media," in *Proceedings of Symposia in Applied Mathematics, Vol. XVI, Stochastic Processes in Mathematical Physics and Engineering*, edited by R. Bellman (American Mathematical Society, Providence, RI, 1964), pp. 145–170.
[25]V. Twerski, "On scattering of waves by random distributions. I. Free-space scatterer formalism," J. Math. Phys. **3**, 700–715 (1962).
[26]V. Twerski, "Acoustic bulk parameters of random volume distributions of small scatterers," J. Acoust. Soc. Am. **36**, 1314–1329 (1964).
[27]V. Twerski, "Acoustic bulk parameters in distributions of pair-correlated scatterers," J. Acoust. Soc. Am. **64**, 1710–1719 (1978).
[28]L-Y Cheng, D. A. Drew, and R. T. Lahey, Jr., "An analysis of wave propagation in bubbly two-component two-phase flow," J. Heat Transfer **107**, 402–408 (1985).
[29]R. Omta, "Oscillations of a cloud of bubbles of small and not so small amplitude," J. Acoust. Soc. Am. **82**, 1018–1033 (1987).
[30]L. d'Agostino and C. E. Brennen, "Acoustical absorption and scattering cross sections of spherical bubble clouds," J. Acoust. Soc. Am. **84**, 2126–2134 (1988).